Calculation of SIFs along a 3-D Crack Front with the Interaction Integral Method Using a Non-Uniform Residual Stress Field

by Ramy Gadallah*, *Student Member* Naoki Osawa*, *Member*
Satoyuki Tanaka**, *Member*

Key Words: *Non-uniform Stress Field, Crack Face Traction, SIFs, Superposition Method, Surface Crack*

1. INTRODUCTION

Welding, nowadays, is widely used in the construction of ships and offshore structures. There is the possibility of flaws (e.g. cracks) being produced from welding. Welding also introduces residual stresses that may influence the strength of a structure. The existence of a crack in a residual stress field is highly risky for a structure integrity [1].

Surface cracks may be found in several structural components and take various shapes, for example, surface cracks in fillet welded joints take the shape of a semi-ellipse. Surface cracks commonly initiate at the regions of stress concentrations such as at the weld toes of fillet joints and may lead to a premature failure of a structure [2,3].

For a reliable prediction of a crack propagation life and fracture strength, accurate stress intensity factor (SIF) solutions are needed for cracked components [2,4]. For ships and offshore structures, surface cracks are frequently found in complicated residual stress fields. It is therefore necessary to take the influence of stress field into account when calculating SIF. In a previous study [5], SIFs were calculated for 3-D surface cracks in a flat plate model and a T-butt welded model including the stress field on the crack face. This study [5] showed that the crack face traction term (CFT-term) must be included in the SIF evaluation technique in order to obtain reliable solutions compared to those given by direct solutions. The authors verified the effectiveness of the CFT-term on the SIF solutions using WARP3D interaction integral method (WARP3D-IIM) for only a flat plate model subjected to tension load (i.e. uniform stress field on the crack face) [5].

This study therefore aims to verify the effectiveness of the CFT-term on the accuracy of SIF solutions using WARP3D-IIM for 3-D surface cracks in a flat plate model and a T-butt welded model when a non-uniform stress field is applied to the crack face. For the sake of comparison, a commercial nonlinear finite element (FE) code (i.e. MSC Marc) that neglects the CFT-term is also used for calculating SIF solutions for the same two models.

2. BACKGROUND

2.1. The Superposition Method

For linear elastic fracture mechanics problems, the superposition method is considered an effective tool for cracks in residual stress fields and cohesive force models. The superposition method is based on that stresses that acting on the boundary of a cracked body can be replaced with traction forces that act on the crack face, where the two loading configurations give the same SIF solution. The SIFs can be calculated for a crack in a complex stress field using the superposition method by dividing the complex loading system into simple cases [4]. The superposition method can only be used for the same loading modes (i.e. modes I, II, or III) [6] and the same displacement boundary conditions.

The superposition method for a semi-elliptical surface cracked body is shown in Fig.1. Based on the superposition method, the SIF ($K_I^{(b)}$) for the body loaded with remote stress (σ) and the crack faces closing stress (-σ) in Fig.1(b) equals zero; because the crack faces are closed and the body behaves as if there is no crack under such conditions [6].

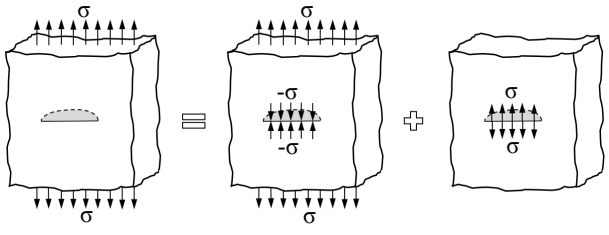

$$K_I^{(a)} = K_I^{(b)} + K_I^{(c)} = K_I^{(c)} \qquad since\ K_I^{(b)} = 0$$

Fig.1 The principle of superposition. (a) a cracked body subjected to a remote tensile loading σ, (b) a geometrically identical uncracked body with the stress field (-σ) in the crack plane produced due to the loading system σ, and (c) a geometrically identical cracked body with crack subjected to the stress field (σ).

2.2. The Domain Integral Method for 3-D Cracks

The domain integral (DI) method is considered a powerful numerical method to calculate the J-integral for 3-D cracks. The general formula of the J-integral requires that the contour surrounding the crack front be very small [6]. The J-integral at location s (see Fig.2) along a 3-D crack front has the general formula [7]:

$$J(s) = \lim_{\Gamma \to 0} \int_{\Gamma} \left(W\delta_{1i} - \sigma_{ij} u_{j,1} \right) n_i d\Gamma, \tag{1}$$

where W is strain energy density, δ_{ij} denotes the Kronecker delta, σ_{ij} is stress components, and u_j represents displacement components. The contour Γ, with normal vector components n_i,

* Graduate School of Engineering, Osaka University
** Graduate School of Engineering, Hiroshima University

Received 25th March 2016
Read at the spring meeting 26th and 27th MAY 2016

exists in X_1–X_2 plane in the local coordinate system, and it starts from the lower crack face and ends at the upper crack face as shown in Fig.2.

Shih et al. [7] formulated Eq. (1) into volume integral and surface integral; to be suitable for numerical analysis in case of 3-D cracks. The energy released per unit advance of crack front segment L_C, $\overline{J}(s)$, is defined as follows:

$$\overline{J}(s)=\int_V\left(\sigma_{ij}u_{j,1}-W\delta_{1i}\right)q_{,i}dV+\int_V\left(\sigma_{ij}u_{j,1}-W\delta_{1i}\right)_{,i}qdV-\int_{S^+ +S^-}t_j u_{j,1}qdS, \tag{2}$$

where t_j are crack face traction components. The volume V consists of cylindrical surfaces (S_1 and S_2), flat lateral surfaces (S_3 and S_4) and upper and lower crack-face surfaces (S^+ and S^-), and surface S_2 shrinks to the crack front (i.e. $r \rightarrow 0$). The weight function q, varies smoothly within volume V. Equation (2) requires that $q = 0$ at S_1, S_3, and S_4 and equals 1.0 at location s on S_2 [7]. The third term in Eq. (2), $\int_{S^+ +S^-}t_j u_{j,1}qdS$, represents the CFT-term.

The second and third terms in Eq. (2) are ignored for elastic, homogenous materials under quasi-static, isothermal loading in case of body forces, thermal strain, and crack face traction are absent in which Eq. (2) gives the identical (volume) DI expression for J [7,8]. The CFT-term, is neglected in commercial nonlinear FE codes (e.g. MSC Marc).

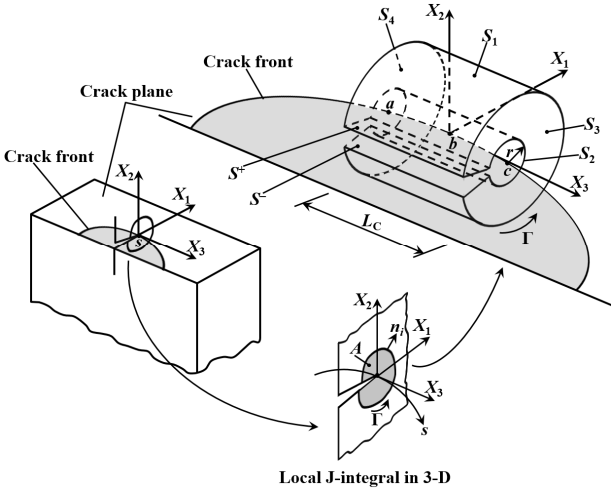

Fig.2 Finite volume (V) for use in DI formulation at crack front location $s = b$ which extends over a segment of the crack front of length L_C from point a to point c.

The approximate formula of the J-integral was derived by Shih et al. [7] by assuming that the energy release rate varies slowly over L_C:

$$J(s)=\frac{\overline{J}(s)}{\int_{L_C}q(s)ds}. \tag{3}$$

The SIFs are valid only for linear-elastic analyses, and assume pure mode-I, mode-II or mode-III loading conditions. The SIF solutions for the three mode conditions (K_I, K_{II} or K_{III}) can be calculated using the J-integral, $J(s)$, in Eq. (3) as follows [9]:

$$K_I=\sqrt{J(s)E^*}\ ,\ K_{II}=\sqrt{J(s)E^*}\ ,\text{ and }\ K_{III}=\sqrt{\frac{J(s)E}{(1+\nu)}}\ , \tag{4}$$

where $E^* = E$ for plane stress condition and $E^* = E / (1 - \nu^2)$ for plane strain condition. As well, E represents Young's modulus and ν denotes Poisson's ratio.

2.3. The Interaction Integral Method for 3-D Cracks

The interaction integral method (IIM) gives actual displacement, stress, and strain fields of an equilibrium state for a boundary value problem. In addition, auxiliary fields that include desired quantities such as SIFs or T-stresses [10,11] can be provided by another selected equilibrium state. A linear combination of actual equilibrium fields with auxiliary fields forms a third equilibrium state called superimposed state. The calculation of the J-integral for this superimposed state leads to a conservation integral, composed of interacting actual and auxiliary terms, that permits direct calculation of SIF [9]. The energy released per unit advance of crack segment for the superimposed state, $\overline{J}^S$, is calculated as follows [8]:

$$\overline{J}^S(s)=\int_V\left[\left(\sigma_{ij}+\sigma_{ij}^{aux}\right)\left(u_{j,1}+u_{j,1}^{aux}\right)-W^S\delta_{1i}\right]q_{,i}dV+\int_V\left[\left(\sigma_{ij}+\sigma_{ij}^{aux}\right)\left(u_{j,1}+u_{j,1}^{aux}\right)-W^S\delta_{1i}\right]_{,i}qdV-\int_{S^+ +S^-}\left(t_j+t_j^{aux}\right)\left(u_{j,1}+u_{j,1}^{aux}\right)qdS. \tag{5}$$

The superscript 'S' denotes the superimposed state. The domain for the interaction integral, $\overline{I}(s)$, defined as [8]:

$$\overline{I}(s)=\int_V\left(\sigma_{ij}u_{j,1}^{aux}+\sigma_{ij}^{aux}u_{j,1}-\sigma_{jk}\varepsilon_{jk}^{aux}\delta_{1i}\right)q_{,i}dV+\int_V\left[\sigma_{ij}\left(u_{j,1i}^{aux}-\varepsilon_{ij,1}^{aux}\right)+\sigma_{ij,1}^{aux}u_{j,1}\right]qdV-\int_{S^+ +S^-}t_j u_{j,1}^{aux}qdS. \tag{6}$$

The third term in Eq. (6), $\int_{S^+ +S^-}t_j u_{j,1}^{aux}qdS$, represents the CFT-term. This term has a significant contribution to the accuracy of the calculated SIF. As for the other quantities in the CFT-term, they do not rely on the FE solution of the boundary value problem [8].

By calculating the value of $\overline{I}(s)$ from Eq. (6), the interaction integral calculation at location s (see Fig.2) over a 3-D crack front follows Eq. (3) as [8]:

$$I(s)=\frac{\overline{I}(s)}{\int_{L_C}q(s)ds}. \tag{7}$$

To extract the SIF at crack front location s for the three loading modes, $I(s)$ defined as [8]:

$$I(s)=\frac{2}{E^*}(K_I K_I^{aux}+K_{II}K_{II}^{aux})+\frac{1}{\mu}(K_{III}K_{III}^{aux}), \tag{8}$$

where $\mu = E/2(1+\nu)$, E^* conditions were defined previously for Eq. (4). By selecting appropriate values for the auxiliary modes of SIFs (K_I^{aux} , K_{II}^{aux} and K_{III}^{aux}) in Eq. (8), relationships between K_I, K_{II}, K_{III} and $I(s)$ can be obtained [8]:

$$K_I=\frac{E^*}{2}I(s)\ ,\ K_{II}=\frac{E^*}{2}I(s)\ ,\text{ and }\ K_{III}=\mu I(s). \tag{9}$$

The selection $K_I^{aux} = 1.0,\ K_{II}^{aux} = K_{III}^{aux} = 0.0$, the selection $K_{II}^{aux} = 1.0,\ K_I^{aux} = K_{III}^{aux} = 0.0$, and the selection $K_{III}^{aux} = 1.0,\ K_I^{aux} = K_{II}^{aux} = 0.0$ in Eq. (8) give the relationships in Eq. (9). To obtain K_I, K_{II} and K_{III} from Eq. (9), the value of $I(s)$ in Eq. (7) is applied. For more details about the IIM, refer to Refs. [8,9].

3. NUMERICAL ANALYSES

3.1. Model Definition

In this study, the SIF solutions for 3-D surface cracks in a flat plat model and a T-butt welded model are evaluated. The geometry of the cracked bodies is shown in Figs. 3 and 4. The cracked T-butt welded body (Fig.4) consists of a one-sided weld with a radiused weld toe as used by Bowness and Lee [12]. The dimensions of surface cracks, crack aspect ratios, and crack depth ratios for each cracked body are shown in Table.1, where a is the crack depth, c is the crack half-length, and t is the model thickness.

Table.1 Crack dimensions (a and c), crack aspect ratios (a/c), and crack depth ratios (a/t) for the flat plate and T-butt welded joint.

Cracked body	a [mm]	c [mm]	a/c	a/t
Flat plate	3.5	9.0	0.39	0.175
T-butt welded joint	3.3	4.7	0.70	0.15

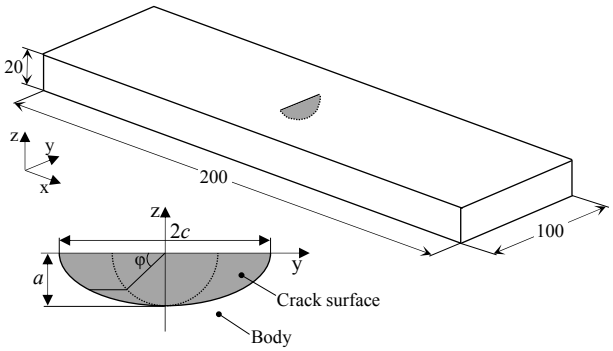

Local coordinates of the surface crack All dimensions in mm

Fig.3 Geometry of the surface cracked flat plate body.

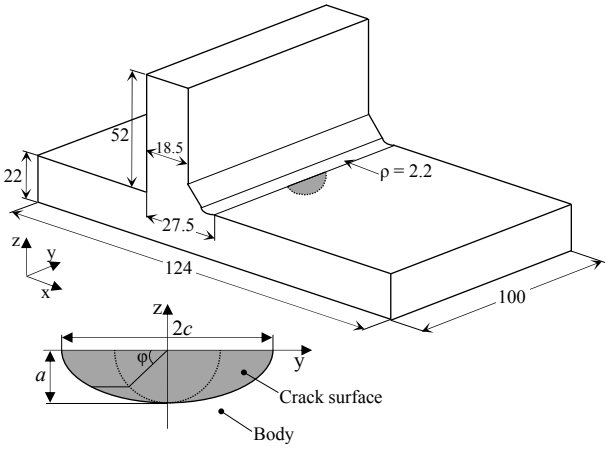

Local coordinates of the surface crack All dimensions in mm

Fig.4 Geometry of the surface cracked T-butt welded body. (Note: ρ is the radius of the weld toe).

The FE models corresponding to Figs. 3 and 4 are shown in Figs. 5 and 6, respectively. Since the cracked bodies are symmetric around the longitudinal axis, one-half symmetric models were used in this study; for the flat plate and T-butt welded joint. The arrows in Figs. 5 and 6 show the applied boundary conditions. The flat plate model and T-butt welded model generated in two steps: 1) create the crack block using Zencrack software [13], and 2) generate the global mesh using Patran software. The crack block then connected to the global mesh. For the T-butt welded model, a FORTRAN program was developed to automatically create the radiused welded toe.

The FE mesh of the cracked models was generated using 20-noded isoparametric hexahedral brick elements. Along the crack front, the 20-noded hexahedral elements are collapsed to quarter-point wedge elements, which are used to simulate the $1/\sqrt{r}$ singularity of the stress field close to the crack front. The Young's modulus and Poisson's ratio used in the analyses are 210 GPa and 0.3, respectively. The rigid body motion of the models is prevented by applying the minimum displacement constraints, as shown in Figs. 5 and 6.

The linear elastic fracture mechanics approach is performed in this study. In this study, the boundary of the flat plate model is subjected to a bending loading. A non-uniform stress field will be introduced on the crack face as a result of such loading. On the other hand, the T-butt welded model is subjected to two separate loading systems. The first loading systems is a uniaxial uniform remote tensile loading in the longitudinal direction, and the other is a bending loading at the boundary of the model. Because of the geometrical parameters of the T-butt welded model such as the shape of the weld bead and weld toe angle, a complex non-uniform residual stress field will arise on the crack face for the two loading configurations. The SIFs for the two models are calculated using the superposition method. To implement the superposition method, two codes are utilized, a commercial nonlinear FE code that will progress the DI method using MSC Marc. The other is an open source research code that will progress the IIM using WARP3D [9]. The CFT-term is neglected in the MSC Marc-DI solution. However, the CFT-term is included in the WARP3D-IIM solution. The WARP3D-IIM solutions will be therefore used to examine the significance of this term on the accuracy of the solutions obtained by crack face traction. The procedure to implement the superposition method is summarized in three steps (see Fig.1):

1) calculation of SIF solutions (K_I values) by applying a remote bending loading for the flat plate model and remote tensile and bending loadings (separate loadings) for the T-butt welded model. The calculated SIF solution in this step is called "direct solution",
2) residual stress field that arises on the crack face is calculated by applying the same remote loading configuration for a geometrically identical uncracked model; and
3) SIF solutions (K_I values) are calculated using a geometrically identical cracked model in which the crack subjected to the stress field that calculated in step 2. The calculated SIF solution in this step is called "crack nodal traction solution" for MSC Marc-DI and is called "crack face traction solution" for WARP3D-IIM.

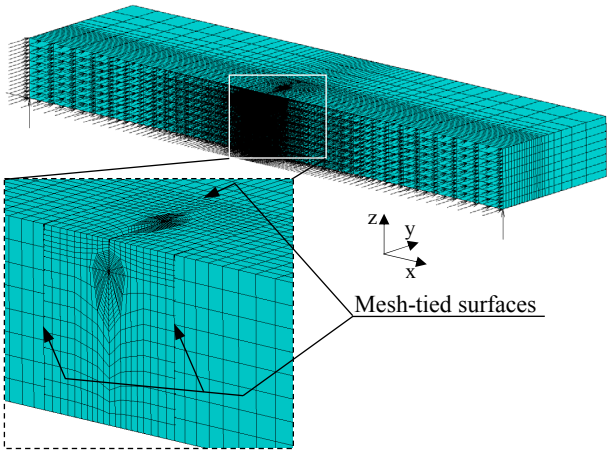

Fig.5 Typical one-half symmetric FE mesh with boundary conditions for the flat plate.

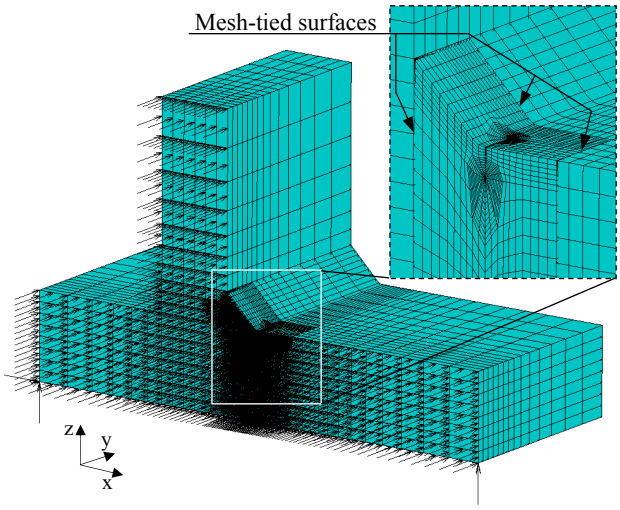

Fig.6 Typical one-half symmetric FE mesh with boundary conditions for the T-butt welded joint.

3.2. Evaluation of SIFs for a Flat Plate Model

In this section, the SIF solutions for a 3-D surface crack in a flat plate model were evaluated using the superposition method. The SIFs were calculated using two different evaluation techniques. The first SIF evaluation technique is MSC Marc using the DI method (i.e. MSC Marc-DI). The other technique is WARP3D using the IMM (i.e. WARP3D-IIM). The MSC Marc solver does not provide the CFT-term in the DI solution. However, the WARP3D code considers the CFT-term in the IIM solution. The crack block was connected to the global mesh using the glue contact option that is offered by MSC Marc and using the tying-mesh option that is available in WARP3D. The SIF direct solutions (K_I values) calculated by MSC Marc-DI and WARP3D-IIM were validated with the solution given by Newman-Raju [14].

When the bending loading was applied to the boundary of the uncracked flat plate model, a non-uniform stress field arose on the crack face. To apply that non-uniform stress field as traction forces on the crack face, the stress field should be properly processed. For MSC Marc, the stress field was calculated as equivalent forces on the crack face nodes. A FORTRAN program was developed to process the generated stress field. The processed stress field was used as a crack nodal traction for the same cracked model that was used for the direct solution except with an opposite sign. For WARP3D, the stress field was calculated as a stress at the element center. Because the size of the elements on the crack face is small; therefore, the stress at the element center can be used as a stress on the element face that exists on the crack face. In the same procedure that done in the case of MSC Marc, the stress field was used as crack face traction for a geometrically identical cracked model. The stress field that applied to the cracked model tries to open the crack (Fig.1 (c)) as in the case of Fig.1 (a). Based on this, the influence of the stress field was included when calculating the SIF solutions (K_I values).

The accuracy of the numerical DI method for the solution obtained by the crack nodal traction was examined by comparing the K_I values calculated by the crack nodal traction with those given by the direct solution. The accuracy of the numerical IIM was also verified for the solution given by the crack face traction with that obtained by the direct solution. To validate the solution for each step of the superposition method (see Fig.1), the total strain energy (U) for the solutions should satisfy Eq. (10). In addition, the crack mouth opening displacement ($CMOD$) for the direct solution and the crack nodal/face traction solution should satisfy Eq. (11). Where U is given in N.mm and $CMOD$ is given in mm. The subscripts (a), (b) and (c) in Eqs. (10) and (11) are based on the three cases in Fig.1. The solutions for the superposition method steps were verified for the MSC Marc-DI and the WARP3D-IIM through Table.2.

$$U_{(a)} = U_{(b)} + U_{(c)}. \tag{10}$$

$$CMOD_{(a)} = CMOD_{(c)}. \tag{11}$$

Table.2 Validation of the solutions for the superposition method steps obtained by the MSC Marc-DI and WARP3D-IIM using the total strain energy (U) and the $CMOD$ for the flat plate model under bending loading.

Case	$U_{(a)}$	$U_{(b)}$	$U_{(c)}$	Difference between $U_{(a)}$ and $U_{(b)} + U_{(c)}$
MSC Marc-DI	1.570e-1	1.567e-1	3.7e-4	0.0003%
WARP3D-IIM	1.593e-1	1.589e-1	4.1e-4	0.0035%
Case	$CMOD_{(a)}$	$CMOD_{(c)}$	Difference between $CMOD_{(a)}$ and $CMOD_{(c)}$	
MSC Marc-DI	6.540e-5	6.541e-5	0.0012%	
WARP3D-IIM	6.908e-5	6.856e-5	0.7542%	

The distribution of the normalized SIFs for mode-I (K_{In}) that calculated by the MSC Marc-DI and the WARP3D-IIM for the flat plate model is shown in Fig.7. Note that, the crack end point and the crack deepest point are represented at $2\varphi/\pi = 0$ and $2\varphi/\pi = 1$, respectively. For MSC Marc-DI solutions (i.e. direct and crack nodal traction solutions), a fairly good agreement between the two solutions was obtained as shown in Fig.7. A difference between the solutions given by MSC Marc-DI was observed. This difference is due to the absence of the CFT-term in the DI solution. The percentage difference between the SIF (K_I value) given by the direct solution and that obtained by the crack nodal traction at the deepest point of the crack (at $2\varphi/\pi = 1$) is 3.4%.

On the other hand, for WARP3D-IIM solutions, an excellent matching between the direct and crack face traction solutions was obtained along the crack front when the CFT-term was included in the IIM solution, except at the crack end. The percentage difference between the SIF (K_I value) given by the direct solution and that obtained by the crack face traction at

the deepest point of the crack is 0.04%. It was observed that when the CFT-term was taken into account, the solution obtained by crack face traction was clearly improved when compared with that given by crack nodal traction.

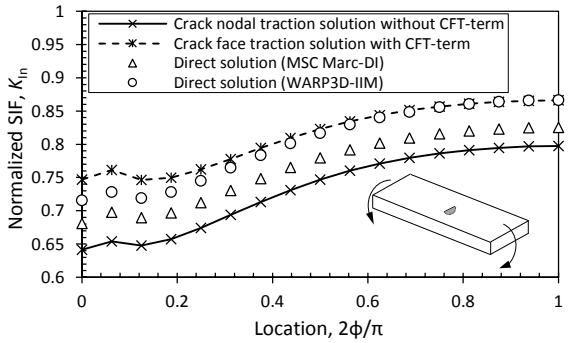

Fig.7 Distribution of the normalized SIFs for mode-I (K_{In}) along the crack front given by the MSC Marc-DI and WARP3D-IIM for the flat plate model under bending loading.

3.3. Evaluation of SIFs for a T-butt Welded Model

For complicated joints such as the T-butt welded joint, a complex stress field, which may be produced by service loading and residual stress, will arise on the crack face. It is therefore necessary to include the influence of residual stress field in the SIF solutions for such joints. This section discusses the application of tensile and bending loading configurations at the boundary of a T-butt welded model, in which the two loading systems will arise a non-uniform residual stress field on the crack face for the uncracked model, as shown in Fig.8. The same SIF evaluation techniques (i.e. MSC Marc-DI and WARP3D-IIM) that used in section 3.2. were also used in this section. The crack block and the global mesh were connected together using the same techniques mentioned in section 3.2. The superposition method was implemented which follows the same sequence that mentioned in section 3.2.

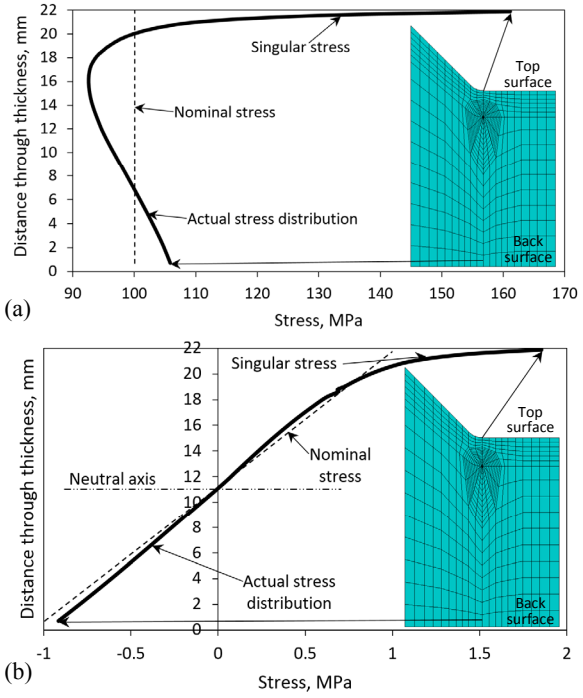

Fig.8 Uncracked weld toe stress distribution. (a) tensile stress and (b) bending stress.

The superposition method steps were verified using Eqs. (10) and (11). The verification of the superposition method steps for the T-butt welded model when subjected to a tensile loading, is shown in Table.3. The solutions for the superposition method steps were also verified when the T-butt welded model subjected to a bending loading, as shown in Table.4.

Table.3 Validation of the solutions for the superposition method steps obtained by the MSC Marc-DI and WARP3D-IIM using the total strain energy (U) and the *CMOD* for the T-butt welded model under tensile loading.

Case	$U_{(a)}$	$U_{(b)}$	$U_{(c)}$	Difference between $U_{(a)}$ and $U_{(b)}+U_{(c)}$
MSC Marc-DI	3.197e+3	3.194e+3	2.5e0	0.0008%
WARP3D-IIM	3.206e+3	3.203e+3	2.4e0	0.0018%
Case	$CMOD_{(a)}$	$CMOD_{(c)}$	Difference between $CMOD_{(a)}$ and $CMOD_{(c)}$	
MSC Marc-DI	5.789e-3	5.951e-3	2.7172%	
WARP3D-IIM	5.811e-3	5.793e-3	0.3166%	

Table.4 Validation of the solutions for the superposition method steps obtained by the MSC Marc-DI and WARP3D-IIM using the total strain energy (U) and the *CMOD* for the T-butt welded model under bending loading.

Case	$U_{(a)}$	$U_{(b)}$	$U_{(c)}$	Difference between $U_{(a)}$ and $U_{(b)}+U_{(c)}$
MSC Marc-DI	9.714e-2	9.690e-2	2.5e-4	0.0002%
WARP3D-IIM	9.908e-2	9.882e-2	2.5e-4	0.0108%
Case	$CMOD_{(a)}$	$CMOD_{(c)}$	Difference between $CMOD_{(a)}$ and $CMOD_{(c)}$	
MSC Marc-DI	5.950e-5	6.179e-5	3.6982%	
WARP3D-IIM	6.088e-5	6.085e-5	0.0558%	

Figure 9 shows the distribution of the normalized SIFs for mode-I (K_{In}) calculated by the direct and the crack nodal/face traction solutions for the T-butt welded model when subjected to a tensile loading. The SIF direct solution obtained by WARP3D-IIM was verified with that given by MSC Marc-DI where an excellent agreement between the direct solutions along the crack front was observed, except at the crack end. The difference obtained at the crack end between the two direct solutions may be due to the influence of the FE modeling. As the SIF at the crack end point strongly depends on the FE modeling and the applied SIF evaluation technique [5].

The solutions given by MSC Marc-DI show a fairly good matching, as shown in Fig.9. Due to the absence of the CFT-term in MSC Marc-DI solution, a difference between the two solutions was observed. For example, a difference of 3.8% was obtained at the crack deepest point between the direct and crack nodal traction solutions. On the other hand, a very good agreement between the solutions given by WARP3D-IIM (i.e. direct and crack face traction solutions) was obtained, as shown in Fig.9. The improvement of the accuracy of the solution calculated by the crack face traction using WARP3D-IIM was due to the implementation of the CFT-term in the IIM. The percentage difference between the direct and crack face traction solutions at the crack deepest point was decreased to be 1.0% when compared to that obtained by MSC Marc-DI.

Figure 10 shows the results of the T-butt welded model under bending loading. Once more, the WARP3D-IIM direct solution was verified with that obtained by MSC Marc-DI. The significance of the CFT-term on the accuracy of the crack

nodal/face traction solution was clear, as shown in Fig.10. For example, for MSC Marc-DI, the percentage difference between the direct and crack nodal traction solutions at the crack deepest point was 2.9%. However, this percentage was clearly decreased for the solutions obtained by WARP3D-IIM at the crack deepest point in which it became 0.2%.

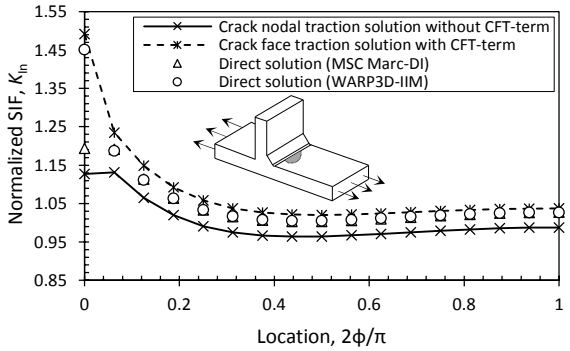

Fig.9 Distribution of the normalized SIFs for mode-I (K_{In}) along the crack front given by the MSC Marc-DI and WARP3D-IIM for the T-butt welded model under tensile loading.

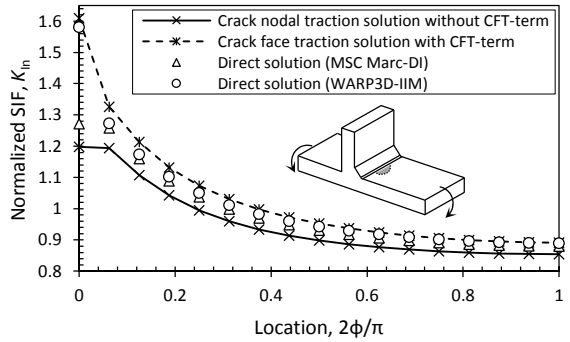

Fig.10 Distribution of the normalized SIFs for mode-I (K_{In}) along the crack front given by the MSC Marc-DI and WARP3D-IIM for the T-butt welded model under bending loading.

3.4. Discussion

It is clear from the results shown in Figs. 7, 9, and 10 that the implementation of the CFT-term in WARP3D-IIM noticeably decreased the difference between the two solutions (i.e. direct and crack face traction solutions), by improving the accuracy of the solutions that obtained by the crack face traction. For example, the CFT-term increased the accuracy of the K_I values given by the crack face traction at the crack deepest point by 26.3% for the T-butt welded model under tensile loading and by 8.0% for the T-butt welded model under bending loading when compared with the accuracy of the crack nodal traction solutions which ignored this term.

It was also observed that the SIF solutions are sensitive to the model mesh. The model mesh should be therefore carefully prepared. On the other hand, the non-uniform stress distributions shown in Fig.8 demonstrate that the proposed technique (i.e. the superposition method and the WARP3D-IIM that includes the CFT-term) in this study is effective when a local stress concentration due to a weld bead is applied to the crack face. This also suggests that the present technique can be used for calculating SIF solutions for a surface crack in a real welding residual stress field.

4. CONCLUDING REMARKS

In this study, the SIF solutions were evaluated for 3-D surface cracks in a flat plate model and a T-butt welded model using the MSC Marc-DI and WARP3D-IIM. A non-uniform stress field was applied to the crack face for the cracked models using the superposition method. Based on the numerical analyses results, the following conclusions can be drawn:

1) The effectiveness of the CFT-term was verified for a flat plate model and a T-butt welded model when a non-uniform stress field was applied to the crack face using the WARP3D-IIM.
2) The CFT-term highly improved the accuracy of the solutions obtained by the crack face traction at the crack deepest point by 26.3% for the T-butt welded model subjected to a tension load and by 8.0% for the T-butt welded model subjected to a bending load when compared to those ignored this term in the MSC Marc-DI.
3) A difference of less than 5% was obtained between the direct and crack nodal traction solutions at the crack deepest point when MSC Marc-DI was used for the two models.
4) The MSC Marc-DI that neglects the CFT-term can be used for engineering fracture problems that subjected to a non-uniform stress field on the crack face under the conditions examined in this study.

5. REFERENCES

1) X.R. Wu and J. Carlsson, Eng. Fracture Mech., Vol. 19, No. 2, pp.407–426, 1984.
2) I.S. Raju, S.N. Atluri, and J.C. Newman, Technical Memorandum No. 100599, NASA, 1984.
3) S. Tanaka, S. Okazawa, H. Okada, Y. Xi, and Y. Ohtsuki, Int. J. Offshore Polar Eng., Vol. 23, No. 3, pp.232–239, 2013.
4) Y.L. Lu, Int. J. Fatigue, Vol. 18, No. 2, pp.127–135, 1996.
5) R. Gadallah, N. Osawa, and S. Tanaka, Proceedings of OMAE2016 (accepted), 2016.
6) T.L. Anderson, 3rd ed., CRC Press, 2005.
7) C.F. Shih, B. Moran, and T. Nakamura, Int. J. Fract., Vol. 130, pp.79–102, 1986.
8) M.C. Walters, G.H. Paulino, and R.H. Dodds, Eng. Fract. Mech., Vol. 72, pp.1635–1663, 2005.
9) B. Healy et al.: WARP3D-release 17.6.0 manual, Report No. UILU-ENG-95-2012, 2015.
10) T. Nakamura, and D.M. Parks, Int. J. Solids Struct., Vol. 29, No. 13, pp.1597−1611, 1992.
11) G.E. Cardew, M.R. Goldthorpe, I.C. Howard, and A.P. Kfouri, Eshelby Memorial Symposium, Cambridge University Press, pp.465−476, 1985.
12) D. Bowness, and M.M.K. Lee, Int. J. Fatigue, Vol. 22, pp.369–387, 2000.
13) Zentech Inc., ZENCRACK 7.2, User's manual, 2003.
14) J.C. Newman and I.S. Raju, NASA TM-85793, 1984.